Inorg. Chem. **2003**, *42*, 3582–3590

Investigations into the Interactions between DNA and Conformationally Constrained Pyridylamineplatinum(II) Analogues of AMD473

Vivienne P. Munk,[†] Connie I. Diakos,[†] Leanne T. Ellis,[†] Ronald R. Fenton,[†] Barbara A. Messerle,[‡] and Trevor W. Hambley*,[†]

Centre for Heavy Metals Research, School of Chemistry, University of Sydney, Sydney, NSW 2006, Australia, and School of Chemical Sciences, University of New South Wales, NSW 2052, Australia

Received January 11, 2003

The syntheses of $[PtCl_2(amp)]$ (amp = 2-pyridylmethylamine) and enantiomerically pure $[PtCl_2(R\text{-pea})]$ and $[PtCl_2(S\text{-pea})]$ (pea = 1-(2-pyridyl)ethylamine) and the crystal structure of $[PtCl_2(R\text{-pea})]$ are reported. The reactions of $[PtCl_2(amp)]$ and of the enantiomers of $[PtCl_2(pea)]$ with d(GpG) and with a 52-base-pair oligonucleotide were investigated. Each of the reactions with d(GpG) resulted in the formation of three platinated bifunctional d(GpG) species in a ratio of 1:2:1. These species were shown to be a pair of isomers, one of which exists as a pair of slowly interconverting rotamers that can be separated by HPLC but reequilibrate after 5 days at 37 °C. The pyridyl moieties of the pyridylalkylamine ligands are constrained to lie in the coordination plane, and as a consequence, the rotation about the Pt–N7 bond of the adjacent guanine is highly restricted. 2D NMR investigations were carried out on the isomer of [Ptd(GpG)(amp)] that did not form separable rotamers and identified it as the isomer having the pyridine adjacent to the 5′-guanine of the d(GpG). The reaction of each of the three $[PtCl_2(py\text{-}R)]$ complexes (py-R = amp or pea) with a 52-base-pair oligonucleotide resulted in the formation of the same three bifunctional d(GpG) adducts in approximately the same ratios as the reactions with d(GpG), indicating that negligible stereoselectivity results from interactions between the complexes and duplex DNA.

Introduction

The cytotoxic activity of the leading anticancer drug cisplatin is believed to derive from direct binding to DNA.[1−7] The limitations of cisplatin have precipitated a search for platinum anticancer drugs that exhibit as much cytotoxic activity as cisplatin but do not exhibit the undesirable side effects.[8−13] In early studies, it was believed that amine ligands with at least one proton were needed for activity, but recently, a considerable amount of interest has been focused on the use of pyridine complexes.[14−18] These studies have shown that the use of bulky planar ligands, such as substituted pyridines, can reduce the rate of deactivation by sulfhydryl groups without interfering with the DNA binding or cytotoxic activity.[16,17] The sterically hindered platinum(II) complex AMD473 (*cis*-$[PtCl_2(NH_3)$(2-methylpyridine)], **1**, see Chart 1) entered clinical trials in November 1997 and has proven to be effective in the treatment of ovarian cancer resistant to carboplatin.[19,20] The drug was designed to overcome

* To whom correspondence should be addressed. E-mail: t.hambley@chem.usyd.edu.au. Phone: 61-2-9351-2830. Fax: 61-2-9351-3329.
[†] University of Sydney.
[‡] University of New South Wales.

(1) Harder, H. C.; Rosenberg, B. *Int. J. Cancer* **1970**, *6*, 207−216.
(2) Howle, J. A.; Gale, G. R. *Biochem. Pharmacol.* **1970**, *19*, 2757−2762.
(3) Reslova, S. *Chem.-Biol. Interact.* **1971**, *4*, 66−70.
(4) Cohen, G. L.; Ledner, J. A.; Lippard, S. J. *J. Am. Chem. Soc.* **1980**, *102*, 2487−2488.
(5) Rosenberg, B. *Cancer* **1985**, *55*, 2303−2314.
(6) Reedijk, J. *Inorg. Chim. Acta* **1992**, *198*−*200*, 873−881.
(7) Zamble, D. B.; Lippard, S. J. *Trends Biochem. Sci.* **1995**, *20*, 435−439.
(8) Cleare, M. J.; Hoeschele, J. D. *Bioinorg. Chem.* **1973**, *2*, 187−210.
(9) Loehrer, P. J.; Einhorn, L. H. *Ann. Intern. Med.* **1984**, *100*, 704−713.
(10) Zwelling, L. A. *Cancer Chemother. Biol. Response Modif.* **1988**, *8*, 64−72.
(11) Kelland, L. R. *Crit. Rev. Oncol./Hematol.* **1993**, *15*, 191−219.
(12) Hambley, T. W. *Coord. Chem. Rev.* **1997**, *166*, 181−223.
(13) Wong, E.; Giandomenico, C. M. *Chem. Rev.* **1999**, *99*, 2451−2466.
(14) van Beusichem, M.; Farrell, N. *Inorg. Chem.* **1992**, *31*, 634−639.
(15) Cusamano, M.; Di Pietro, M. L.; Giannetto, A. *J. Chem. Soc., Chem. Commun.* **1996**, 2527−2528.
(16) Holford, J.; Raynaud, F.; Murrer, B. A.; Grimaldi, K.; Hartley, J. A.; Abrams, M.; Kelland, L. R. *Anti-Cancer Drug Des.* **1998**, *13*, 1−18.
(17) Hay, M. *Curr. Opin. Oncol. Endocr. Metab. Invest. Drugs* **1999**, *1*, 443−447.
(18) Okada, T.; El-Mehasseb, I. M.; Kodaka, M.; Tomohiro, T.; Okamoto, K.-I.; Okuno, H. *J. Med. Chem.* **2001**, *44*, 4661−4667.

10.1021/ic0340231 CCC: $25.00
Published on Web 05/09/2003

Chart 1

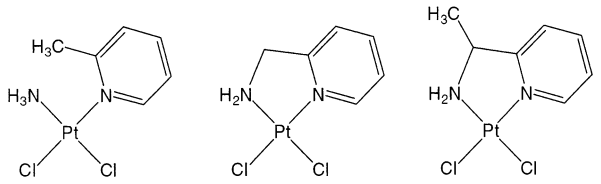

1 **2** **3**

resistance caused by cytoplasmic thiols, such as glutathione and metallothionein.[16,17]

Recent studies have shown that steric effects can play an important role in controlling the binding of bulky platinum complexes to DNA.[21−24] Chen and co-workers have reported that the binding of AMD473 to DNA is also influenced by steric factors.[25,26] In this present work, we have investigated the interactions between platinum complexes related to AMD473 and DNA. The complex [$PtCl_2$(amp)] (**2**) can be thought of as an analogue of AMD473, with a methylene chain linking the pyridine ring to the amine, constraining the pyridine group to lie in the coordination plane. This removes the steric bulk that lies above the coordination plane of AMD473 and is believed to contribute to many of its novel properties. Thus, a comparison of the behavior of [$PtCl_2$-(amp)] and AMD473 will shed light on the effects of this steric bulk. The complex [$PtCl_2$(pea)] (**3**) has, in addition, a methyl group bound to the methylene chain, generating a chiral carbon and the possibility of enantioselective interactions.

In this study, the stereoselectivity of the interactions of these constrained pyridyl platinum complexes with d(GpG) and a 52-mer DNA fragment has been investigated using digestion, HPLC, molecular modeling, and NMR.

Experimental Section

Materials. $K_2[PtCl_4]$ was purchased from Aithaca Chemical Corp., 2-deoxyguanylyl(3′-5′)-2-deoxyguanosine (d(GpG) was purchased from Sigma-Aldrich, 2-pyridylmethylamine was purchased from Strem, and the double stranded oligonucleotide (52-mer) containing 6-GpG sites was synthesized by Sigma Genosys. HPLC grade solvents for HPLC separation were purchased from Selby Biolab.

Instrumentation. Polarimetry measurements were carried out on an Optical Activity POLAAR 2001 dual wavelength automatic polarimeter, using a 1 dm cell at ambient temperature. A JASCO J-710 spectropolarimeter equipped with J-700 software for Windows was used for circular dichroism measurements. Diffuse reflectance infrared Fourier transform spectra (DRIFTS) were collected in a potassium bromide matrix, over the range 400−4000 cm^{-1} on a Bio-Rad FTS-40 spectrophotometer, equipped with Win-IR software. ^1H and ^{13}C NMR spectroscopy was carried out on a Bruker AC 200 MHz spectrometer or a Bruker AMX 400 MHz spectrometer, using commercially available solvents. All spectra were referenced to an internal standard (tms or tps) or to solvent isotopic impurities. 2D NMR spectra were collected on a Bruker Avance DMX 600 MHz spectrometer. HPLC analysis was performed on a Bio-Rad Series 800 HRLC gradient system using v2.30.1a software. The system was fitted with a Bio-Rad model 2800 solvent delivery system, a Bio-Rad UV-1806 UV−vis detector, and a Bio-Rad model 2110 fraction collector. The samples were chromatographed on an Alltech Platinum C-18 (5 μm particle size, 4.6 mm × 250 mm) analytical column, using an acetonitrile gradient in TEAA (triethylammonium acetate, 20 mM, pH 7). Platinum concentrations were determined using a Varian SpectrAA-20 graphite furnace atomic absorption spectrometer (GFAAS), equipped with a GTA-96 graphite tube atomizer and a PC-56 autosampling system. GFAAS readings were measured between 0 and 302.7 ppb Pt in a HCl matrix.

Synthesis of 2-Pyridylmethylamineplatinum(II). Literature methods were adapted for the synthesis of [$PtCl_2$(amp)].[27,28] A sample of $K_2[PtCl_4]$ (200 mg, 0.48 mmol) was added to a solution of 2-pyridylmethylamine (amp) (52 mg, 0.48 mmol) in 5 mL of water. The solution was stirred at room temperature in the dark for 3 h and filtered at the pump and the solid product washed with ethanol and diethyl ether. The platinum complex was characterized by IR and NMR spectroscopy. ^1H NMR ppm (δ): 4.45 (m, 2H); 7.52 (m, 1H); 7.67 (m, 1H); 8.21 (m, 1H); 9.24 (m, 1H). Yield: 0.14 g, 0.37 mmol, 77%.

Synthesis of 1-(2-Pyridyl)ethylamineplatinum(II). The synthesis and resolution of 2-pyridylethylamine (pea) was carried out as reported previously.[29−31] A novel method was used for the synthesis of the platinum complexes. Optically pure pea (0.05 g, 0.4 mmol) in 100 mL of acidified water (2 drops, concentrated HCl) was added to a solution containing $K_2[PtCl_4]$ (0.17 g, 0.4 mmol), sodium chloride (0.54 g), and water (700 mL). The solution was slowly evaporated in an oven at 45 °C. After 7 days, clear yellow needles had formed, and the solid was filtered at the pump, washed with ice-cold water, and air-dried. The filtrate was returned to the oven, and a second crop was collected at the pump after a further 3 days. The platinum complexes were characterized by NMR, IR, and CD polarimetry. ^1H NMR ppm (δ): 1.42 (m, 3H); 4.11 (m, 1H); 7.11 (t, 1H); 7.34 (d, 1H); 7.65 (t, 1H); 8.52 (d, 1H). ^{13}C NMR ppm (δ): 24.2 (s, CH_3); 52.2 (s, CH); 119.7 (s, aroC); 121.4 (s, aroC); 136.3 (s, aroC); 148.8 (s, aroC); 165.5 (s, aroC). Yields: *R* 79 mg, 0.20 mmol, 50%, and *S* 72 mg, 0.11 mmol, 46%. The CD spectra have been deposited as part of the Supporting Information.

Structure Determination. Crystals of [$PtCl_2$(*R*-pea)] were grown from a solution of [$PtCl_2$(*R*-pea)] in H_2O at 45 °C, and a suitable crystal was selected and mounted onto a glass fiber. The data were obtained at room temperature with a Bruker SMART 1000 CCD diffractometer using graphite monochromated Mo Kα radiation

(19) Raynaud, F. I.; Boxall, F. E.; Goddard, P. M.; Valenti, M.; Jones, M.; Murrer, B. A.; Abrams, M.; Kelland, L. R. *Clin. Cancer Res.* **1997**, *3*, 22063−2074.
(20) Kelland, L. R.; Sharp, S. Y.; O'Neill, C. F.; Raynaud, F. I.; Beale, P. J.; Judson, I. R. *J. Inorg. Biochem.* **1999**, *77*, 111−115.
(21) Ling, E. C. H.; Allen, G. W.; Hambley, T. W. *J. Am. Chem. Soc.* **1994**, *116*, 2673−2674.
(22) Hambley, T. W.; Ling, E. C. H.; Messerle, B. A. *Inorg. Chem.* **1996**, *35*, 4663−4668.
(23) Hambley, T. W.; Ling, E. C. H.; Munk, V. P.; Davies, M. S. *J. Biol. Inorg. Chem.* **2001**, *6*, 534−542.
(24) Munk, V. P.; Diakos, C. I.; Messerle, B. A.; Fenton, R. R.; Hambley, T. W. *Chem. Eur. J.* **2002**, *8*, 5486−5493.
(25) Chen, Y.; Guo, Z.; Parsons, S.; Sadler, P. J. *Chem. Eur. J.* **1998**, *4*, 672−676.
(26) Chen, Y.; Guo, Z. J.; Parkinson, J. A.; Sadler, P. J. *J. Chem. Soc., Dalton Trans.* **1998**, 3577−3585.
(27) Niven, M. L.; Percy, G. C.; Thornton, D. A. *J. Mol. Struct.* **1980**, *68*, 73−80.
(28) Brunner, H.; Schmidt, M.; Schonenberger, H. *Inorg. Chim. Acta* **1986**, *123*, 201−207.
(29) Smith, H. E.; Schaad, L. J.; Banks, R. B.; Wiant, C. J.; Jordan, C. F. *J. Am. Chem. Soc.* **1973**, *95*, 811−818.
(30) Michelsen, K. *Acta Chem. Scand.* **1974**, *28*, 428−434.
(31) Bang, E. *Acta Chem. Scand. A* **1977**, *31*, 495−500.

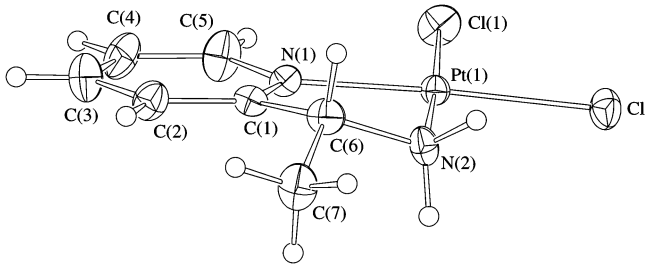

Figure 1. ORTEP plot of [$PtCl_2$(*R*-pea)] giving the crystallographic atom numbering. 30% probability ellipsoids are shown.

Table 1. Crystallographic Details for [$PtCl_2$(*R*-pea)]

empirical formula	$PtC_7H_{10}N_2Cl_2$
fw	388.17
space group	$P2_12_12_1$
a, Å	6.9137(6)
b, Å	14.975(1)
c, Å	9.4432(9)
V (Å^3)	977.7(1)
Z	4
μ, mm^{-1}	147.86
ρ_{obsd}, g cm^{-3}	2.637
T, K	293
λ, Å	0.71073
$R(F_o)$	0.028
R_w	0.039

generated from a sealed tube. An empirical absorption correction determined with SADABS[32] was applied to the data. The data integration and reduction were undertaken with SAINT and XPREP and included the application of Lorentz and polarization corrections.[33] Crystallographic details are summarized in Table 1.

The structure was solved by direct methods using SHELXS-86[34] and refined using full-matrix least-squares methods with teXsan.[35] Hydrogen atoms were included at calculated sites with isotropic thermal parameters fixed at 1.5 times those of the parent atoms. Non-hydrogen atoms were refined anisotropically. Scattering factors and anomalous dispersion terms for Pt were taken from International Tables.[36] Anomalous dispersion effects were included in F_c;[37] the values for $\Delta f'$ and $\Delta f''$ were those of Creagh and McAuley.[38] The values for the mass attenuation coefficients are those of Creagh and Hubbell.[39] All other calculations were performed using the teXsan[35] crystallographic software package of Molecular Structure Corporation. The atomic nomenclature is defined on the ORTEP[40] plot in Figure 1. Listings of atom coordinates, complete tables of bond lengths, angles and torsion angles, anisotropic thermal parameters, and details of least-squares planes calculations have been deposited and are given as part of the Supporting Information.

Reaction of the Platinum Complexes with d(GpG). The preparation of the bifunctional Pt/d(GpG) adducts was carried out using a method adapted from published procedures.[41,42] Freshly dissolved [$PtCl_2$(amp)], [$PtCl_2$(*R*-pea)], or [$PtCl_2$(*S*-pea)] (1.34 mM, 149 μL) was reacted with equimolar amounts of d(GpG) (Sigma, 5 mM, 40 μL) in sterile aqueous sodium perchlorate (0.1 M, pH 5.5). The samples were incubated at 37 °C for 7 days and stored at −20 °C until required for HPLC analysis.

Larger Scale Preparation of [Ptd(GpG)(amp)] for NMR Analysis. Large scale samples of [Ptd(GpG)(amp)] for 600 MHz NMR analysis were prepared following an adapted literature method.[22,24] A freshly dissolved solution of [$PtCl_2$(amp)] (5 mM, 1.294 mL) was reacted with an equimolar amount of d(GpG) (5 mM, 1.294 mL). Both reactants were dissolved in sterile aqueous sodium perchlorate (0.02 M, pH 5.5). The samples were incubated at 37 °C for 7 days and stored at −20 °C prior to HPLC separation.

Reactions of Platinum Complexes with a 52-mer Duplex Oligonucleotide. A 52-base-pair (bp) self-complementary oligonucleotide with the sequence 5′TAATTGGTATATTGGTATATAC-CAATATTGGTATATACCAATATACCAATTA3′ was annealed and treated with the platinum complexes, following a procedure adapted from several literature methods.[43−47] To anneal the DNA, the oligonucleotide (1640 μg, sodium salt) was dissolved in 1 mL of high purity water and then denatured by heating at 95 °C for 5 min. The DNA was then slowly renatured by stepwise cooling. The oligonucleotide was incubated at 65 °C for 10 min, 37 °C for 30 min, 65 °C for 10 min, and 37 °C for 4 h and then slowly cooled to room temperature. The annealed oligonucleotide was stored at −20 °C until time of use.

The annealed 52-bp oligonucleotide (Sigma, 100 μg) was incubated for 7 days at 37 °C with freshly dissolved [$PtCl_2$(amp)], [$PtCl_2$(*R*-pea)], or [$PtCl_2$(*S*-pea)] (1 mM in 0.02 M $NaClO_4$, pH 5.5, 92.37 μL) at an R_t value equaling 0.05. The platinated DNA was then digested with P_1 nuclease (40 μg, Type EC 3.1.30.1 in 50% 20 mM sodium acetate, 50% glycerol solution, pH 5.5, Sigma) at 37 °C for 16 h. Tris buffer (1 M, pH 9, 40 μL) was added, and the samples were incubated with alkaline phosphatase (10 U, in 2.5 M ammonium sulfate solution, Sigma) for a further 4 h at 37 °C. The digested DNA was then freeze-dried, resuspended in aqueous sodium perchlorate (0.02 M. pH 5.5, 200 μL), and stored at −20 °C prior to HPLC analysis.

NMR Spectroscopy of an Isomer of [Ptd(GpG)(amp)]. NMR experiments were carried out with a ca. 1 mM solution of [Ptd(GpG)(amp)] (peak B) in D_2O. Spectra were collected over a spectral width of 6000 Hz; quadrature detection was employed throughout. The ^{1}H 1D and 2D data were acquired using water presaturation. Homonuclear ^{1}H 2D (DQF)COSY and ROESY (τ_m = 200 ms) spectra were acquired in phase-sensitive mode with time-proportional phase incrementation. 2D spectra were acquired using standard Bruker pulse sequences. For the COSY spectrum, data sets resulting from 512 t_1 increments were acquired with each free

(32) Sheldrick, G. M. *SADABS, Area detector absorption and other corrections*, version 2.0; Bruker/Siemens: Madison, WI, 2000.
(33) *SMART, SAINT and XPREP, Area detector control and data integration and reduction software*; Bruker Analytical X-ray Instruments Inc.: Madison, WI, 1995.
(34) Sheldrick, G. M. In *Crystallographic Computing 3*; Sheldrick, G. M., Krüger, C., Goddard, R., Eds.; Oxford University Press: Oxford, 1986; pp 175−189.
(35) *teXsan, Crystal Structure Analysis Package*; Molecular Science Corporation: The Woodlands, TX, 1985 and 1992.
(36) Cromer, D. T.; Waber, J. T. *International Tables for X-ray Crystallography*; Kynoch Press: Birmingham, U.K., 1974; Vol. 4.
(37) Ibers, J. A.; Hamilton, W. C. *Acta Crystallogr.* **1964**, *17*, 781.
(38) Creagh, D. C.; McAuley, W. J. *International Tables for Crysallography*; Wilson, A. J. C., Ed.; Kluwer Academic Publishers: Boston, 1992; Vol. C, pp 219−222, Table 4.2.6.8.
(39) Creagh, D. C.; Hubbell, J. H. *International Tables for Crysallography*; Kluwer Academic Press: Boston, 1992; Vol. C, Table 4.2.4.3.
(40) Johnson, C. K. *ORTEP, A Thermal Ellipsoid Plotting Program*; Oak Ridge National Laboratories: Oak Ridge, TN, 1965.
(41) Eastman, A. *Biochemistry* **1983**, *22*, 3927−3933.
(42) Eastman, A. *Biochemistry* **1985**, *24*, 5027−5032.
(43) Fichtinger-Schepman, A. M. J.; Lohman, P. H. M.; Reedijk, J. *Nucleic Acids Res.* **1982**, *10*, 5345−5356.
(44) Fichtinger-Schepman, A. J.; van der Veer, J. L.; den Hartog, J. H. J.; Lohman, P. H. M.; Reedijk, J. *Biochemistry* **1985**, *24*, 707−713.
(45) Eastman, A. *Biochemistry* **1986**, *25*, 3912−3915.
(46) Eastman, A.; Jennerwein, M. M.; Nagel, D. L. *Chem.-Biol. Interact.* **1988**, *67*, 71−80.
(47) Ling, E. C. H. Ph.D. Thesis, University of Sydney, Sydney, 1995, p 191.

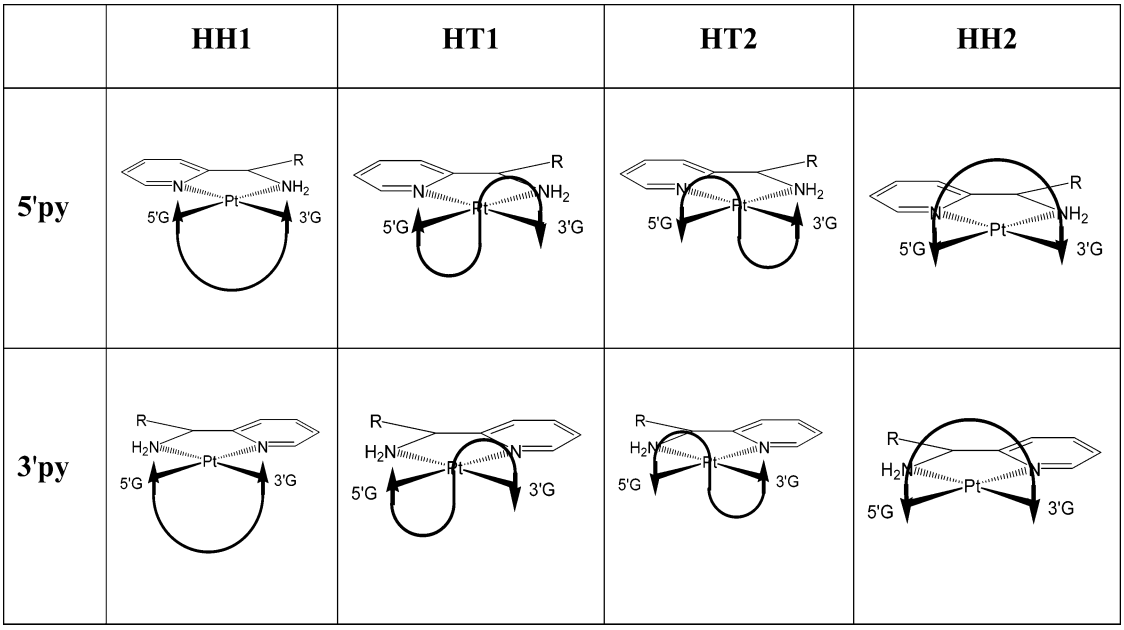

Figure 2. Isomers and rotamers of [Ptd(GpG)(py-R)]. The head of the arrows represent the direction toward the H8 for each guanine.

induction decay composed of 2048 data points, using a recycle delay of 1.8 s. The ROESY spectrum was acquired with 512 t_1 increments, with a recycle delay of 1.6 s and the free induction decay composed of 2048 data points. All data was subjected to shifted sine-bell weighting functions in F1 and F2 of $\lambda/2$ and baseline corrected using Bruker software. Spectra were processed using Bruker XWinNMR software, version 2.6. Referencing of all data was made internally to TEAA.

Molecular Mechanics Calculations. Starting models for molecular modeling were generated using HYPERCHEM and energy-minimized using MOMECSG-95.[48] Force fields have been previously published,[49−52] and all models were subjected to energy minimization using MOMECSG-95 until convergence was achieved (all shifts < 0.01 Å). The DNA fragment used for modeling was an 8-mer duplex with the sequence GGG**G*G***GGG:CCCCCCCC, with the platinum binding via the N7 atoms of the two guanines marked with asterisks. The models were then energy minimized until constant energy (±1 kJ mol^{-1}) was achieved.

Results and Discussion

Synthesis of Platinum(II) Complexes. The synthesis of [$PtCl_2$(amp)] was readily achieved, with the ligand coordinating to platinum in aqueous solution in relatively high yields. The novel technique of slow evaporation at constant temperature (45 °C) of an aqueous solution containing platinum ions, the ligand, and excess chloride ions was used for the synthesis of the enantiomers of [$PtCl_2$(pea)], with the platinum complexes also forming in relatively high yield. Circular dichroism spectra of the [$PtCl_2$(pea)] enantiomers had equal but opposite absorption profiles.

Crystal Structure. The ORTEP plot of [$PtCl_2$(*R*-pea)] (Figure 1) shows a square-planar geometry around the platinum, with bidentate chelation of the *R*-pea ligand. The complex is largely planar with the pyridyl ring lying at an angle of only 7.9° to the coordination plane. The methylene carbon, C(6), lies only 0.12 Å out of the pyridyl plane, and the chelate ring N−C−C−N torsion angle is −22.2(9)°. The methyl group lies in an equatorial position which is somewhat suprising since it results in a close contact between it and the pyridine (H···H 2.16 Å) that would not be present if the methyl group were in the axial position. The more planar geometry of the equatorial conformer may be favored by crystal packing. Pt−Cl and Pt−N bond lengths are normal with no significant difference between the lengths of the bonds to the amine and pyridine moieties (2.026(5) and 2.030(5) Å, respectively).

Reactions of Platinum(II) Complexes with d(GpG). Two isomers are expected to form in the reaction of the amp and pea platinum(II) complexes with d(GpG): one isomer with the pyridine ring adjacent to the 5′ guanine (5′py, Figure 2) and the second with the pyridine ring adjacent to the 3′ guanine (3′py, Figure 2). It has been shown that the adducts that form between platinum(II) complexes and d(GpG) can adopt up to four conformations.[53−55] The most frequently observed is the head-to-head (HH1; *anti*, *anti*), in which the H8 protons of the guanines are oriented in the same direction. Head-to-tail (HT) cross-links, in which the H8 protons are oriented in opposite directions, can be either an *anti*, *syn* (HT1) or a *syn*, *anti* (HT2) orientation. The fourth observed orientation of bifunctional d(GpG) adducts (HH2; *anti*, *anti*) is not common. Consequently, for unsymmetrical platinum complexes, such as those in this study, eight configurations

(48) Hambley, T. W.; Comba, P. *MOMEC-95: A program for strain energy minimisation package adapted to Hyperchem*; 1995.
(49) Hambley, T. W. *Inorg. Chem.* **1988**, *27*, 1073−1077.
(50) Hambley, T. W. *Inorg. Chem.* **1991**, *30*, 937−942.
(51) Ling, E. C. H.; Allen, G. W.; Hambley, T. W. *J. Chem. Soc., Dalton Trans.* **1993**, 3705−3710.
(52) Hambley, T. W. *Inorg. Chem.* **1998**, *37*, 3767−3774.
(53) Kozelka, J.; Fouchet, M.-H.; Chottard, J.-C. *Eur. J. Biochem.* **1992**, *205*, 895−906.
(54) Ano, S. O.; Kuklenyik, Z.; Marzilli, L. G. In *Cisplatin: Chemistry and Biochemistry of a Leading Anticancer Drug*; Lippert, B., Ed.; Verlag Helvetica Chimica Acta; Wiley-VCH: Zurich and Weinheim, 1999; pp 247−291.
(55) Marzilli, L. G.; Ano, S.; Intini, F. P.; Natile, G. *J. Am. Chem. Soc.* **1999**, *121*, 9133−9142.

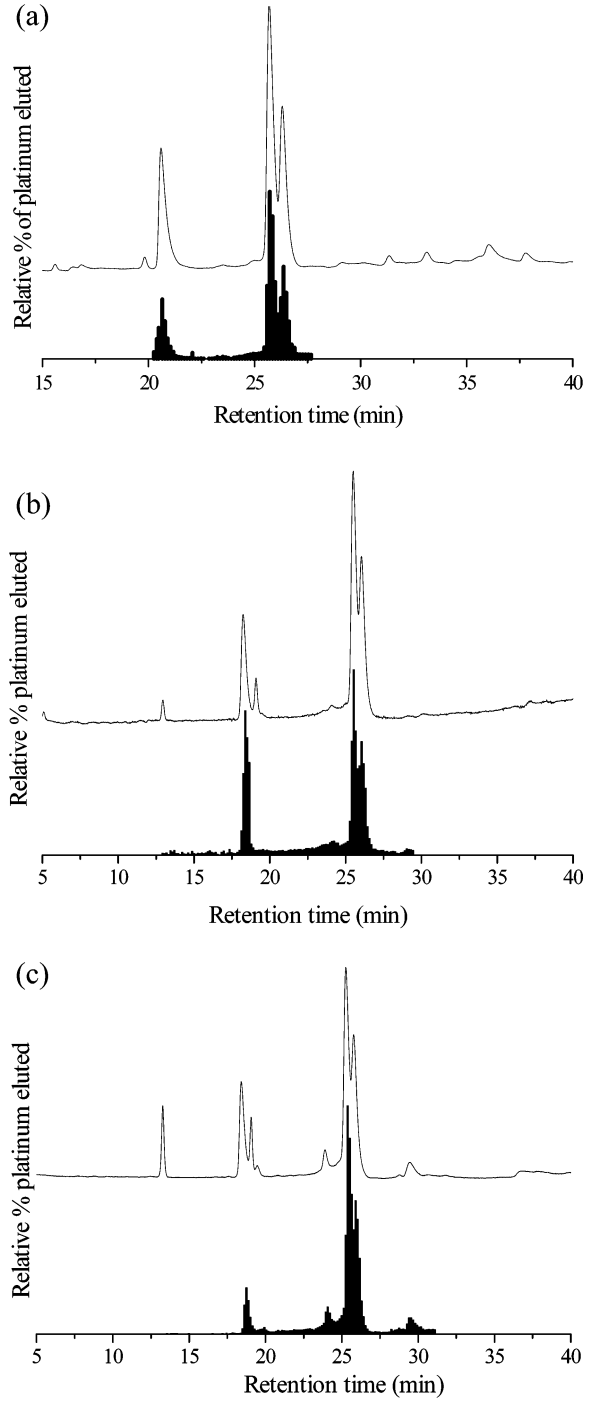

Figure 3. HPLC chromatogram and platinum profile for the products of the reaction between d(GpG) and (a) [$PtCl_2$(amp)], (b) [$PtCl_2$(*R*-pea)], and (c) [$PtCl_2$(*S*-pea)].

are possible, four for each isomer (Figure 2). The isomers, 5′py and 3′py, are expected to be separable, but rotamers usually interconvert too rapidly to be isolated.[54,55]

Figure 3 shows the HPLC chromatograms and platinum profiles for the products of the reactions of d(GpG) with [$PtCl_2$(amp)] and with each of the enantiomers of [$PtCl_2$-(pea)]. Three major product peaks are observed in each chromatogram, one more than expected for two isomers. In addition, [$PtCl_2$(*S*-pea)] formed two minor platinated peaks, possibly due to monofunctionally bound species.

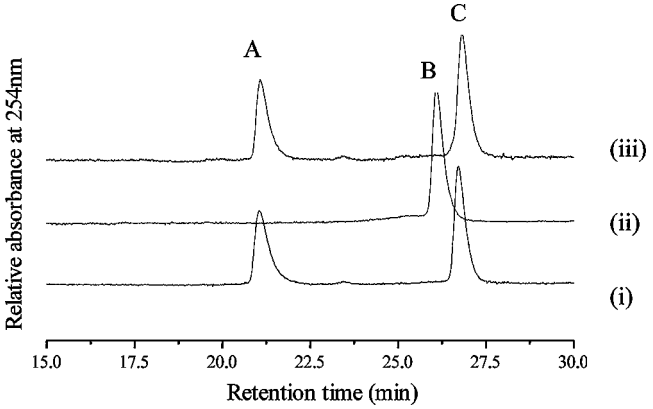

Figure 4. HPLC chromatograms for the incubated and rechromatographed bands from the reaction between [$PtCl_2$(amp)] and d(GpG) (Figure 3a) showing that (i) band A gives rise to bands A and C, (ii) band B gives only band B, and (iii) band C gives rise to bands A and C.

Table 2. Calculated Total Strain Energies (kJ mol^{-1}) for the HH1 and HT Models of [$PtCl_2$(amp)]

rotamer	HH1	HH1	HT1	HT1	HT2	HT2
isomer	**5′py**	**3′py**	**5′py**	**3′py**	**5′py**	**3′py**
energy ($kJ\ mol^{-1}$)	−175.0	−172.9	−185.1	−188.8	−186.2	−186.0

For the reaction of d(GpG) and [$PtCl_2$(amp)], each peak (labeled A, B, and C corresponding to the order of elution from the HPLC) was collected and reincubated at 37 °C for 5 days. After this time, each fraction was rechromatographed, and the resulting chromatograms are shown in Figure 4. On equilibration, peak A formed two peaks (A and C), peak B remained as a single peak (B), and peak C formed two peaks (A and C). We postulate therefore, that peaks A and C are due to slowly interconverting rotamers, that differ in the orientation (*syn* or *anti*) of the guanine adjacent to the pyridine (Figure 2). These rotamers can be separated by HPLC because the pyridyl group restricts the rotation of the adjacent guanine about the Pt−N7 bond, but they are able to interconvert on warming for a few days.

Molecular Modeling of the Platinum Adducts Formed with d(GpG). HH and HT models were generated for all of the [Ptd(GpG)(amp)] isomers and rotamers. The calculated strain energies for the energy-minimized models are given in Table 2 and reveal that the HT rotamers are more stable than the HH. The isomers of each rotamer differ in energy by only less than 4 kJ mol^{-1}, probably within the error range in calculations of this type.

Figure 5 shows the molecular models for the HH1 isomers of [Ptd(GpG)(amp)]. No significantly destabilizing contacts are observed between the ligand and the dinucleotide for the HH models of [Ptd(GpG)(amp)].

NMR Spectroscopy. 2D NMR spectroscopy of the second HPLC peak (peak B) eluted from the products of the reaction between [$PtCl_2$(amp)] and d(GpG) was used to identify it on the basis of cross-peaks between the resonances due to the amp ligand and those due to d(GpG). Peak B eluted as only a single peak when the incubated sample was rechromatographed, which led us to believe that it contained only one conformer of [Ptd(GpG)(amp)] or that it contained a

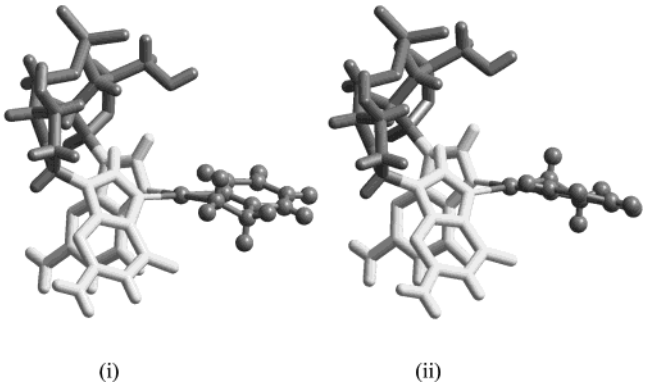

Figure 5. Molecular models of the head-to-head rotamers of the isomers of [Ptd(GpG)(amp)]. Isomer 5′py (i) has the pyridine ring adjacent to the 5′ guanine, and isomer 3′py (ii) has the pyridine ring adjacent to the 3′ guanine.

second conformer that exchanged too rapidly to be separated by HPLC. A bulk sample of peak B was purified by HPLC, lyophilized, and dissolved in D_2O in an NMR tube for analysis using 600 MHz NMR spectroscopy. The results of an NMR pH titration experiment have been included in the Supporting Information and confirm that the platinum complex is bound to the guanines via the N7 atoms, as indicated by inflection points at approximately pH 8.5.[56−58] Resonances of the ligand and sugar protons were assigned using 2D COSY, ROESY, and phosphorus−proton correlation techniques. Only one set of resonances was observed in the 2D NMR spectra, and thus it was concluded that peak B contained only one conformer of [Ptd(GpG)(amp)] or a mixture of conformers rapidly interconverting on the NMR time scale. 2D COSY spectra were used to assign the proton chemical shifts (Table 3). Through space interactions between the dinucleotide and the amp ligand were probed using 2D ROESY experiments, Figure 6, and all of the observed H8 cross-peaks are given in Table 4. A cross-peak between the resonances due to the H8a (5′ guanine) and H8b (3′ guanine) protons implies that these protons are in close proximity, suggesting that the guanines are predominantly in a HH

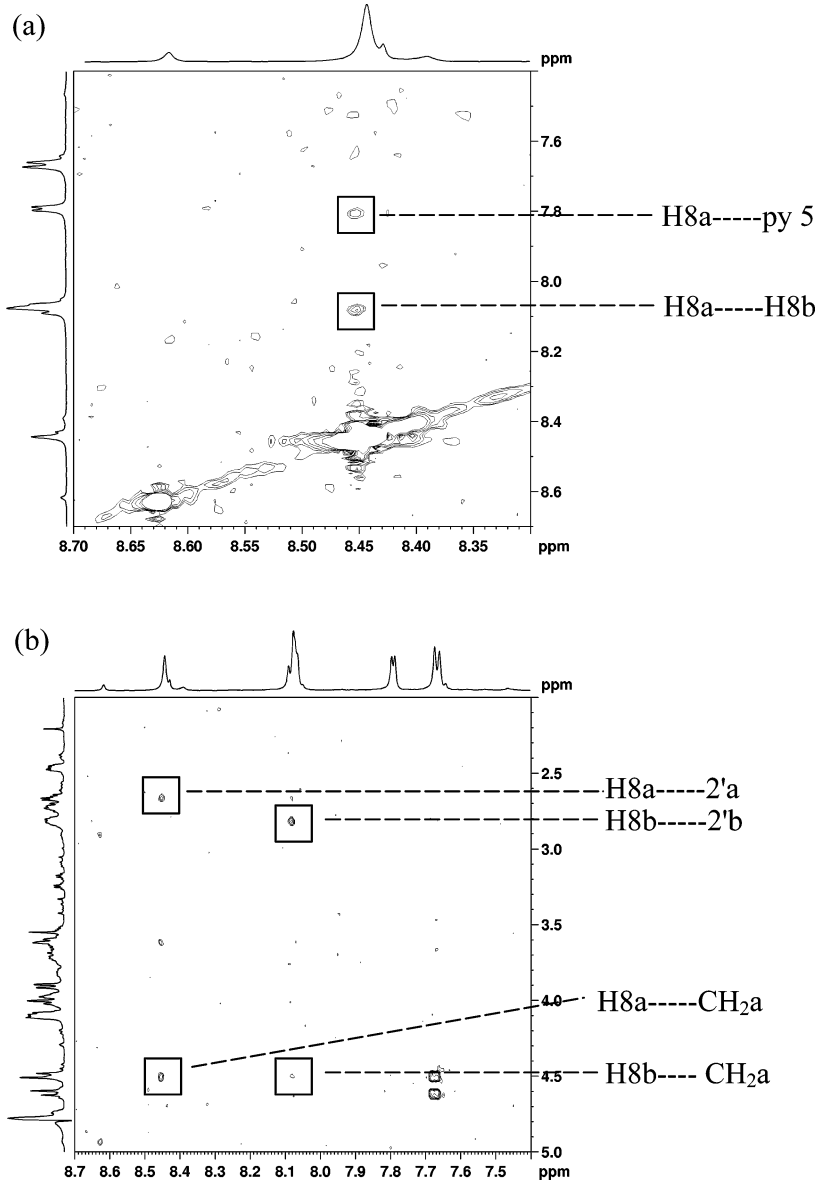

Figure 6. Through space interactions for (a) pyridine···H8 region and (b) H8···sugar/CH_2 region.

Table 3. Chemical Shifts for the Sugar and Ligand Regions of Peak B

proton	chemical shift (ppm)	proton	chemical shift (ppm)
1′a	6.29	py 2	7.68
1′b	6.15	py 3	8.08
2′a	2.69	py 4	7.24
2″a	2.75	py 4	7.80
2′b	2.85	CH_2a	4.50
2″b	2.49	CH_2b	4.61
3′a	4.52		
3′b	4.75	H8a	8.45
4′a	4.13	H8b	8.08
4′b	4.15		
5′a	3.92		
5″a	3.64		
5′b	4.02		
5″b	4.00		

Table 4. Cross-Peaks Seen in the ROESY Spectrum for the H8 Protons of Peak B

ROESY cross-peak	relative strength	ROESY cross-peak	relative strength
H8a···H8b	2.54 (M)	H8b···′b	17.32 (S)
H8a···py 5	3.05 (M)	H8b[a]···CH_2a	2.49 (W)
H8a···1′a	3.09 (M)	H8b[a]···CH_2b	2.23 (W)
H8a···CH_2a	7.17 (S)	H8b[a]···2′b	0.80 (W)
H8a···3′a	2.07 (W)	H8b[a]···2″b	8.14 (S)
H8a···2′a	6.38 (S)		

[a] Resonances due to the H8b and py 3 protons overlap, and thus, either proton may be involved in this interaction

Table 5. H8 Contacts in the HH Models of [Ptd(GpG)(amp)][a]

interaction	isomer 5′py	isomer 3′py
H8a···CH_2a	6.04	5.43
H8a···CH_2b	6.28	5.44
H8a···py 2	7.73	7.30
H8a···py 3	6.55	8.33
H8a···py 4	**4.83**	7.59
H8a···py 5	**2.62**	5.49
H8b···CH_2a	6.14	6.38
H8b···CH_2b	6.44	6.77
H8b···py 2	7.90	7.78
H8b···py 3	8.55	8.02
H8b···py 4	7.37	6.49
H8b···py 5	**5.06**	**4.13**
H8a···H8b	**3.03**	**3.03**

[a] Interactions detectable in ROESY NMR experiments are shown in bold.

conformation. Thus, a comparison between the interactions seen in the energy-minimized HH models of [Ptd(GpG)(amp)] and the NMR ROESY cross-peaks was used to identify peak B. The H8 distances are given in Table 5, and the contacts which would be detected by ROESY experiments have been highlighted. The 2D ROESY experiments reveal through space interactions between the resonances of the H8a protons and the py 5 and CH_2 protons of the ligand. The cross-peak between the resonances due to H8a and CH_2a is relatively intense, but it is difficult to conceive how a contact as close as that implied by the intensity of this cross-peak could arise. Therefore, we attribute this cross-peak to an unusual spin-diffusion process. The contact between the py 5 proton and H8a indicates that peak B corresponds to isomer 5′py because only this isomer has a close contact (2.62 Å) between these atoms. No other strong cross-peaks are expected for this isomer, and the 2D spectrum is inconsistent with isomer 3′py for which a cross-peak between py 5 and H8b would be expected.

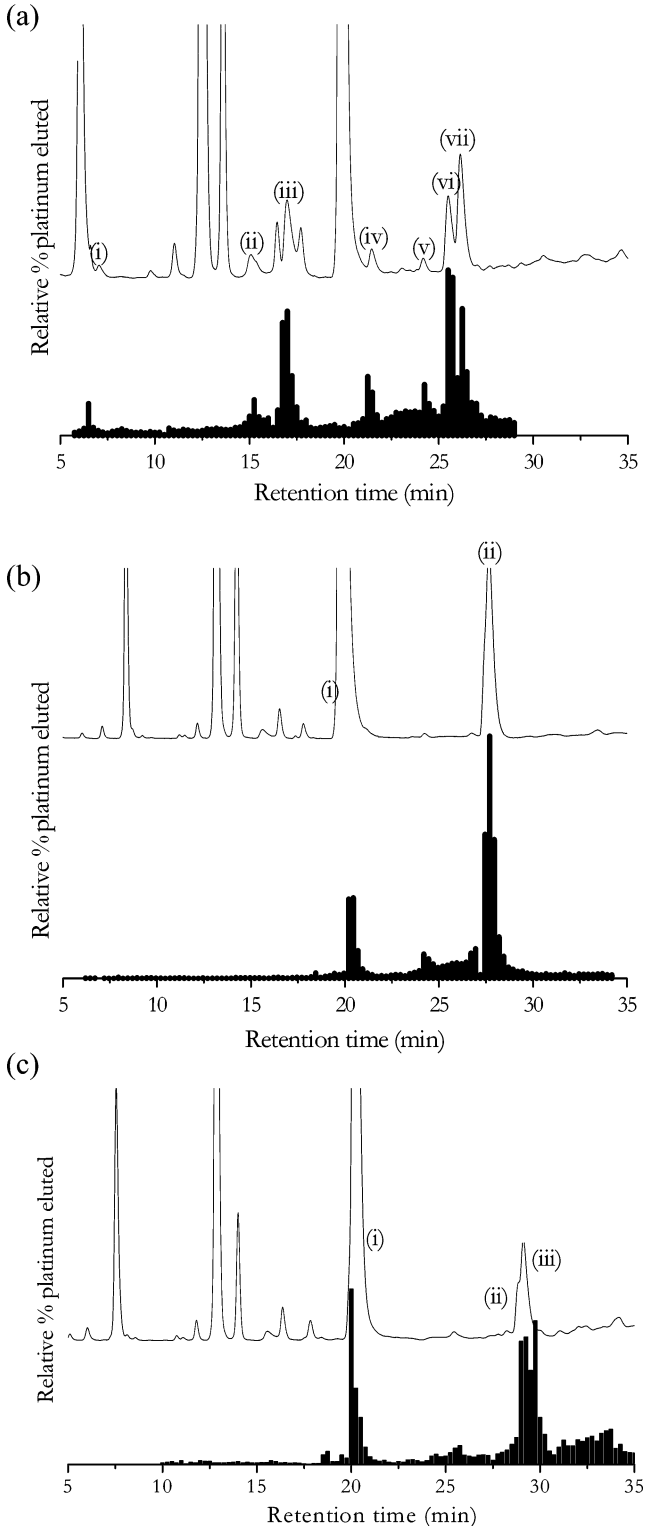

Figure 7. HPLC chromatogram and platinum profile for the products of the reaction between a 52-base-pair oligonucleotide and (a) [$PtCl_2$(amp)], (b) [$PtCl_2$(*R*-pea)], and (c) [$PtCl_2$(*S*-pea)].

Reactions of Platinum Complexes with a Duplex 52-Mer. Figure 7 shows the HPLC chromatograms and platinum profiles for the digested products of [Pt(52-mer)(amp)], [Pt-(52-mer)(*R*-pea)], and [Pt(52-mer)(*S*-pea)]. The four major

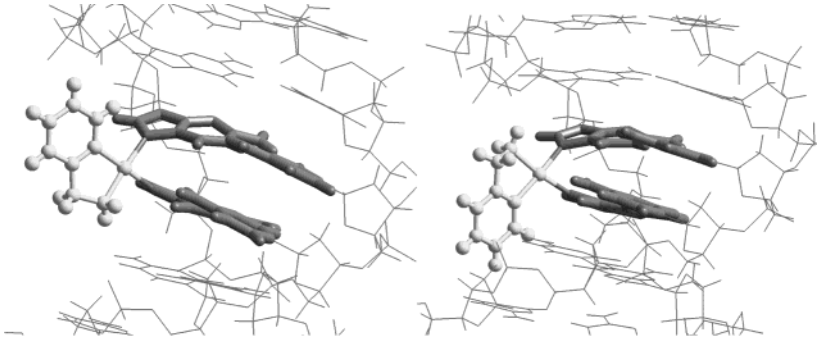

Figure 8. Molecular models of the isomers of [Pt(8-mer)(amp)]. Isomer 5′py (i) has the pyridine ring adjacent to the 5′ end of the adduct, and isomer 3′py (ii) has the pyridine ring adjacent to the 3′ end.

peaks observed in each chromatogram correspond to unplatinated nucleosides (dC, dG, dT, and dA). There are also between three and seven peaks that contain platinum in each elution profile. The reaction mixtures were spiked with the [Ptd(GpG)(py-R)] standards, and the resulting chromatograms have been deposited as part of the Supporting Information. These spiking experiments confirmed that the major platinated species formed were [Ptd(GpG)(py-R)] products, arising from bifunctional binding to the DNA. In the HPLC chromatograms of the digestion products of [Pt(52-mer)(amp)], it can be seen that seven platinum containing peaks are eluted. The three major peaks (labeled iii, vi, and vii) correspond to the three bifunctional [Ptd(GpG)(amp)] species (A, B, and C) seen in the reaction between d(GpG) and [$PtCl_2$(amp)], and they are formed in similar ratios, with peaks iii and vii forming at a slightly higher level. These two peaks were identified as interconverting rotamers, and therefore, the concomitant increase in both peaks is to be expected. The minor peaks have not been identified, but they are most likely to correspond to monofunctional adducts.

Two major platinated peaks were observed in the digestion products of [Pt(52-mer)(*R*-pea)] (peaks i and ii), compared with three platinum containing peaks in the reaction of [$PtCl_2$-(*R*-pea)] and d(GpG). From the shape of peak ii, it can be seen that two peaks (B and C) have coeluted. Slightly differing retention times and resolutions may have been caused by the different reaction matrix and reaction conditions, and in accord with this, upon spiking with the three peaks of the d(GpG) standard, only two peaks are observed. Three major platinum containing peaks (i, ii, and iii) are seen in the digestion products of [Pt(52-mer)(*S*-pea)], which were identified as [Ptd(GpG)(*S*-pea)] species (A, B, and C). These three peaks were also formed in similar ratios in the reaction of d(GpG) and [$PtCl_2$(*S*-pea)]; however, peak B forms in a slightly lower proportion in the reaction with duplex DNA.

It can be seen that the binding profiles of [$PtCl_2$(py-R)] with d(GpG) and duplex DNA are very similar, which suggests that neither the length of the nucleotide nor the duplex structure significantly influences the formation of bifunctional GpG adducts by these complexes.

Molecular Modeling of the Platinum Adducts Formed with Duplex DNA. Molecular modeling of the isomers formed between the [$PtCl_2$(amp)] and an eight-base-pair oligonucleotide (G8) was carried out to visualize the interactions between the complexes and double stranded DNA. Figure 8 shows the molecular models of the two isomers of [Pt(8-mer)(amp)] in which the pyridine ring is disposed toward either the 5′ end or the 3′ end of the DNA. When cisplatin binds to GpG sequences, the NH_3 groups are able to form hydrogen bonds with the phosphate on the 5′ side of the adduct and/or the O6 of the 3′ guanine. The NH_2 group of the amp ligand can form similar hydrogen bonds, but only that to O6 is possible for isomer 5′py and only that to the phosphate for isomer 3′py. Other than these contacts, the methylamine moiety makes no close contacts with the DNA. However, the pyridine group does make some close contacts. In the case of isomer 5′py, these H···H contacts of about 2.6 Å are to the sugar on the 5′ side of the adduct, and in the case of 3′py, they are similar length contacts to the cytosine bases on the 3′ side of the adduct. None of these interactions are particularly destabilizing, and this is reflected in the relatively undistorted geometry about platinum. In previous studies, we have shown that the N7−Pt−N(amine) angles provide a good indication of the extent of destabilizing interactions between the complex and DNA.[23,24] The chelate ring and N7−Pt−N7 angles are usually 75−85°, and therefore, the "unstrained" N7−Pt−N(amine) angles are 97−100°. Here, these angles are opened up very slightly with the N7−Pt−N(pyridine) angle 103° in isomer 5′py and 106° in isomer 3′py. Thus, they are consistent with the observation of moderately unfavorable contacts between the pyridine and the DNA and suggest that these interactions may be slightly more destabilizing for isomer 3′py.

Conclusions

The conformationally constrained pyridyl platinum(II) complexes studied form three major platinated species in a ratio of approximately 1:2:1 when reacted with d(GpG). When isolated, the first and third of these species re-equilibrate to give a mixture of the same two species, with the second peak eluting remaining as a single peak following

(56) Girault, J.-P.; Chottard, G.; Chottard, J.-C.; Lallemand, J.-Y. *Biochemistry* **1982**, *21*, 1352−1356.
(57) Dijt, F. J.; Canters, G. W.; den Hartog, J. H. J.; Marcelis, A. T. M.; Reedijk, J. *J. Am. Chem. Soc.* **1984**, *106*, 3644−3647.
(58) Lemaire, D.; Fouchet, M.-H.; Kozelka, J. *J. Inorg. Biochem.* **1994**, *53*, 261−271.

incubation. 2D NMR experiments of the second peak (peak B) for [Ptd(GpG)(amp)] have identified this adduct as isomer 5′py, which has the pyridine ring adjacent to the 5′guanine. The species that re-equilibrate have been postulated to be rotational isomers that form due to the rotation about the Pt−N7 bond, and it is easy to envisage that the pyridine ligand, constrained as it is to lie close to the coordination plane, prevents the adjacent guanine from readily rotating about the Pt−N7 bond. It is not clear why only a single rotamer is observed for isomer 5′py. Either one rotamer is greatly preferred over the other or this isomer is permanently trapped as a single rotamer. The separable rotamers of isomer 3′py are most likely HH1 and HT1 since conversion from HH1 to HT2 involves rotation of the guanine adjacent to the NH_2 moiety and this is likely to occur very readily. The difference between the strain energies of these HH1 and HT1 rotamers is 15.9 kJ mol^{-1} whereas that between the expected rotamers for isomer 5′py (HH1 and HT2) is less at 11.2 kJ mol^{-1}. Thus, it is unlikely that a greater preference for a single rotamer is responsible for the observations of a single peak for isomer 5′py. Trapping of a single rotamer would be surprising given the relative ease with which the rotamers of isomer 3′py interconvert, but it is the most plausible explanation at present.

No clear stereoselectivity is observed in the interactions between the constrained platinum complexes and duplex DNA. This is consistent with the molecular modeling studies which show that there are only moderately unfavorable interactions between the amp ligand and the DNA and there are only slight differences between these interactions for the two isomers. This contrasts with the situation for AMD473 where high stereoselectivity has been reported.[59]

Acknowledgment. The support of the Australian Research Council and the Sydney University Cancer Research Fund is gratefully acknowledged.

Supporting Information Available: Crystallographic data and additional figures. This material is available free of charge via the Internet at http://pubs.acs.org.

IC0340231

(59) Chen, Y.; Parkinson, J. A.; Guo, Z. J.; Brown, T.; Sadler, P. J. *Angew. Chem., Int. Ed.* **1999**, *38*, 2060−2063.